Korean J. Chem. Eng., 35(8), 1726-1734 (2018)
DOI: 10.1007/s11814-018-0061-5

pISSN: 0256-1115
eISSN: 1975-7220

Photocatalysis assisted by activated-carbon-impregnated magnetite composite for removal of cephalexin from aqueous solution

Forough Gashtasbi*,, Reza Jalilzadeh Yengejeh**,†, and Ali Akbar Babaei***,****

*Department of Environmental Engineering, Khuzestan Science and Research Branch, Islamic Azad University, Ahvaz, Iran
**Department of Environmental Engineering, Ahvaz Branch, Islamic Azad University, Ahvaz, Iran
***Environmental Technologies Research Center, Ahvaz Jundishapur University of Medical Sciences, Ahvaz, Iran
****Department of Environmental Health Engineering, School of Public Health,
Ahvaz Jundishapur University of Medical Sciences, Ahvaz, Iran
(*Received 8 December 2017 • accepted 5 April 2018*)

Abstract−The simultaneous presence of antibiotics and bacteria in aqueous media has been recognized as an environmental threat, due to the enhancement of antibiotic resistance of bacteria. We synthesized an activated carbon impregnated magnetite composite (PAC/Fe_3O_4) and used it for removal of cephalexin (CEX) from aqueous solution via UV system. A series of batch experiments was carried out under various experimental conditions such as pH of solution (3-11), contact time (0-120 min), catalyst dosages (0.1-2 g/L) and initial CEX concentrations (10, 25, 50 and 100 mg/L). Some common isotherm models were used for study of CEX adsorption and finding the best model. In addition, kinetic studies of CEX photocatalytic removal were performed by fitting the experimental data on first-order and second-order models. Results of comparative studies showed that UV+PAC/Fe_3O_4 and UV+TiO_2 systems, compared to UV/Fe_3O_4, naked Fe_3O_4, PAC/Fe_3O_4 and UV only, had more capability of removing CEX from aqueous solution, indicating PAC/Fe_3O_4 is effectively catalyzed by UV light. Furthermore, increasing catalyst dosages and decreasing initial CEX concentrations led to the enhancing photocatalytic removal of CEX from solution. The obtained results of kinetic studies also represent that among the studied models, second-order model with significant coefficient of correlation (R^2) had higher ability than first-order model to fit the data of CEX removal. Finally, the findings of reusability tests, showed that the applied catalyst would be applicable for CEX removal, even after five consecutive cycles.

Keywords: Cephalexin, Kinetic, Reusability, Magnetic Composite, UV System

INTRODUCTION

Regarding the fast growth and development of manufacturers, pharmaceutical drugs like antibiotics used in different industries, stock farming and bio-manufacturing have been discharged into the water bodies and posed a serious threat for human life. Among the antibiotics, cephalosporins are considered as the most extensively applied antibiotics, which are categorized in four principal branches according to their antimicrobial activities. Cephalexin (CEX) is known as the first-generation applied cephalosporin antibiotic and used on a large scale for infections in humans and animals [1]. Recently, a huge volume of CEX was discharged into the water resources without being applied by live organisms. CEX is very resistant against degradation and can remain in aqueous media for a long period. Therefore, it is quite necessary to employ an efficient and innovative technique for its removal from solution.

Different remediation techniques such as reduction [2], Fenton-oxidation [3], biosorption [4], photocatalysis [5] and adsorption [6] have been utilized for treating water contaminated with pharmaceutical substances. However, the application of these treatment approaches has not represented fruitful results, due to the low antibiotic removal efficiency, high cost of operation and leaving secondary pollution. Therefore, a cost-effective and highly efficient remediation techniques has to be employed for removal of antibiotics from aqueous solution. Photocatalysis has gained the attention of environmentalists and been applied in previous studies for remediation of solution from many contaminants, which represented high performance [7-9].

In previous decades, many authors have focused their attentions on titanium dioxide (TiO_2), as a semiconductor typical photocatalyst, owing to its excellent features such as strong oxidizing power, chemical stability, ease of availability and low cost and low toxicity [10,11]. However, separation and recovery problem from the liquid phase has limited the practical use of TiO_2 in real applications. To overcome this problem, researchers applied photocatalysts with magnetic properties. Fe_3O_4 has been reported as an efficient photocatalyst in the degradation of pollutants [12,13]. It is well-known that when Fe_3O_4 faced with UV light can generate a reactive species such as hydroxyl radicals (HO•), according to reactions 1-3 [14]:

$$Fe_3O_4 + h\nu \rightarrow h_{VB^+} + e_{CB^-} \qquad \lambda < 400\ nm \tag{1}$$

$$Fe_3O_4(h_{VB^+}) + H_2O \rightarrow {}^{\bullet}OH + H^+ \tag{2}$$

$$h_{VB^+} + H_2O \rightarrow {}^{\bullet}OH_{(ads)} + H^+ \tag{3}$$

Fe_3O_4 nanoparticles also could be separated and recycled conve-

†To whom correspondence should be addressed.
E-mail: r.jalilzadeh@iauahvaz.ac.ir

niently by applying an external magnetic field. However, the strong tendency for Fe_3O_4 nanoparticles to agglomerate is a major concern for application and can decrease the surface area, reactivity and removal efficiency. The incorporated Fe_3O_4 nanoparticles into the porous supporting materials such as graphene, zeolite, activated carbon and polymeric materials can be a useful approach for resolving this problem [15]. Hence, an activated carbon impregnated magnetite composite (PAC/Fe_3O_4) has been fabricated which not only has high ability of adsorbing pollutants, but also can be easily catalyzed by UV light as well as separated from solution, due to its magnetic features [14].

Although the study of CEX removal using photocatalysis method has been conducted, the application of magnetic composite for increasing the performance of a photocatalytic system requires more consideration. Therefore, we synthesized a magnetic activated carbon composite and used it for photocatalytic removal of CEX from solution. To the best of our knowledge, no study has been reported for CEX photocatalytic removal by PAC/Fe_3O_4 composite. The performance of photocatalyst process was evaluated at different experimental factors of solution pH, catalyst dosages and initial CEX concentrations. In addition, the kinetic study of CEX photocatalytic removal was also carried out using three most common models.

MATERIALS AND METHODS

1. Reagents

To synthesize PAC/Fe_3O_4, ferric nitrate ($Fe(NO_3)_3{\cdot}9H_2O$), activated carbon powder, ammonia and nitric acid were purchased from Merck, Co, Germany. Cephalexin powder was prepared from Jaberebne Ghayyan drug company, Iran.

2. Preparation and Characterization of Composite

The composite was prepared using co-precipitation method, proposed by [16]. At first step, 5 g of activated carbon powder was added to 20 mL 65% nitric acid solution. Then, for homogenizing the suspension, it was put in an ultrasonic bath for 3 h at 80 °C. Then, samples were filtered and dried at room temperature. Subsequently, 5 g of obtained powder was impregnated into a 200 mL of aqueous solution containing $Fe(NO_3)_3{\cdot}9H_2O$ and placed in ultrasonic vibration for 1 h at 80 °C. After filtration, they were dried in an electrical furnace at 750 °C during a 3 h time period under N_2 gas flow. In the final step, the synthesized composite was rinsed with DI water for several times and dried in an oven at 105 °C and then kept in a desiccator, until beginning the experiments.

The size, morphology and surface features of the synthesized composite were evaluated using a scanning electron microscope (SEM, Philips, XL30). The crystalline characteristics of PAC/Fe_3O_4 were also studied using X-ray diffraction (XRD,) instrument at 2θ of 10-80°. The elemental analysis of the surface of PAC/Fe_3O_4 involved using energy dispersive X-ray (EDX) technique. In addition, the surface area of the sample was calculated using Brunauer-Emmett-Teller (BET) method through adsorption-desorption of N_2.

3. Experimental Procedure

The removal of CEX using UV+PAC/Fe_3O_4 used two processes of adsorption and photocatalysis. In brief, for performing batch adsorption experiments, some certain dosages of adsorbent (0.1-2 g/L) were added to plastic bottles containing solution with different initial CEX concentrations (5, 10, 25, 50 mg/L). Then, they were shaken vigorously on a rotary shaker at different time periods. First, batch adsorption experiments were done at 120 min; since no significant changes were happened in the adsorption of CEX after 60 min, this time period was selected as an equilibrium time for next experiments. After ending reaction, the adsorbent particles were separated using an external magnet to find the residual CEX concentrations in the solution. In addition, equilibrium and kinetic studies of batch experiment were performed using different widely applied models.

Furthermore, to carry out photocatalytic experiments of CEX removal, 100 mL of 25 mg/L CEX solution was placed into the 250 mL quartz flask, which was sealed with aluminum foil. For homogenizing the composite and effective mass transfer in the reactor, the suspension was stirred vigorously using a stirrer with high intensity. A UV lamp with (UV-C lamp, 6W PHILIPS) and 254 nm wavelength peaking was put into the open central region of the sample.

After a defined time interval, the residual CEX concentration in aqueous solution was determined using a UV-visible spectrophotometer (HACH, DR-5000) at wavelength of 261 nm and the photocatalytic removal of CEX (R %) was calculated using the equation below:

$$R = \frac{C_o - C}{C_o} \times 100 \tag{4}$$

where, C_o and C are the initial and residual CEX concentrations (mg/L), respectively.

4. Isotherm Studies

The maximum amount of monolayer adsorption capacity (q_m) was obtained by fitting the Langmuir equation as follows. The essential features of the Langmuir isotherm may be expressed in terms of equilibrium parameter R_L, which is a dimensionless constant referred to as separation factor or equilibrium parameter [17]:

$$\frac{1}{q_e} = \frac{1}{q_m} + \frac{1}{q_m K_L C_e} \tag{5}$$

$$R_L = \frac{1}{1 + (1 + K_L C_o)} \tag{6}$$

The experimental data were also fit to the Freundlich model, which assumes the heterogeneous nature of adsorption. The linear form of Freundlich isotherm model is expressed as follows [18]:

$$\ln q_e = \ln K_F + \frac{1}{n} \ln C_e \tag{7}$$

Based on Temkin isotherm model assumption, the linear decrease happens in the adsorption energy with surfaces coverage, which is derived from the interactions between adsorbent and adsorbate molecules. Eq. (5) shows the linear form of Temkin isotherm model [19]:

$$q_e = \frac{RT}{A_T} \ln K_T + \frac{RT}{A_T} \ln C_e \tag{8}$$

The Dubinin-Radushkevich (D-R) model is used for adsorption mechanism with a Gaussian energy distribution onto a heteroge-

neous surface. This model is also applicable for physical adsorption processes [20]:

$$\ln q_e = \ln q_s - k_{ad}\varepsilon^2 \quad (9)$$

where, q_e and C_e are the adsorption capacity of adsorbent (mg/g) and residual adsorbate concentration (mg/L).

5. Photocatalytic Degradation Kinetic Studies

For better explanation of the photocatalytic removal of CEX, the experimental data were fitted on the two most common kinetic models: first-order and second-order models. Eq. (10) shows the first-order kinetic model, which is known as the most widely applied model in remediation processes, as follows [21]:

$$C_t = C_o \exp(-k_1 t) \quad (10)$$

The second-order model is given via the following equation:

$$\frac{1}{C_o} - \frac{1}{C_t} = -k_2 t \quad (11)$$

where, t is reaction time (min), C_o and C_t are the initial and residual concentrations of CEX (mg/L) at time t and k_1 (min^{-1}) and k_2 ($mg^{-1}\cdot L\cdot min^{-1}$) are the rate constants of first-order and second-order models, respectively.

RESULTS AND DISCUSSION

1. Characterization

SEM image of PAC/Fe_3O_4 is illustrated in Fig. 1(a) and (b) that shows the surface characteristics of the synthesized composite. Having a closer look, it has some surface roughness and cavities with various sizes and shapes which provide huge capability of adsorbing contaminants. XRD diagram of the synthesized composite,

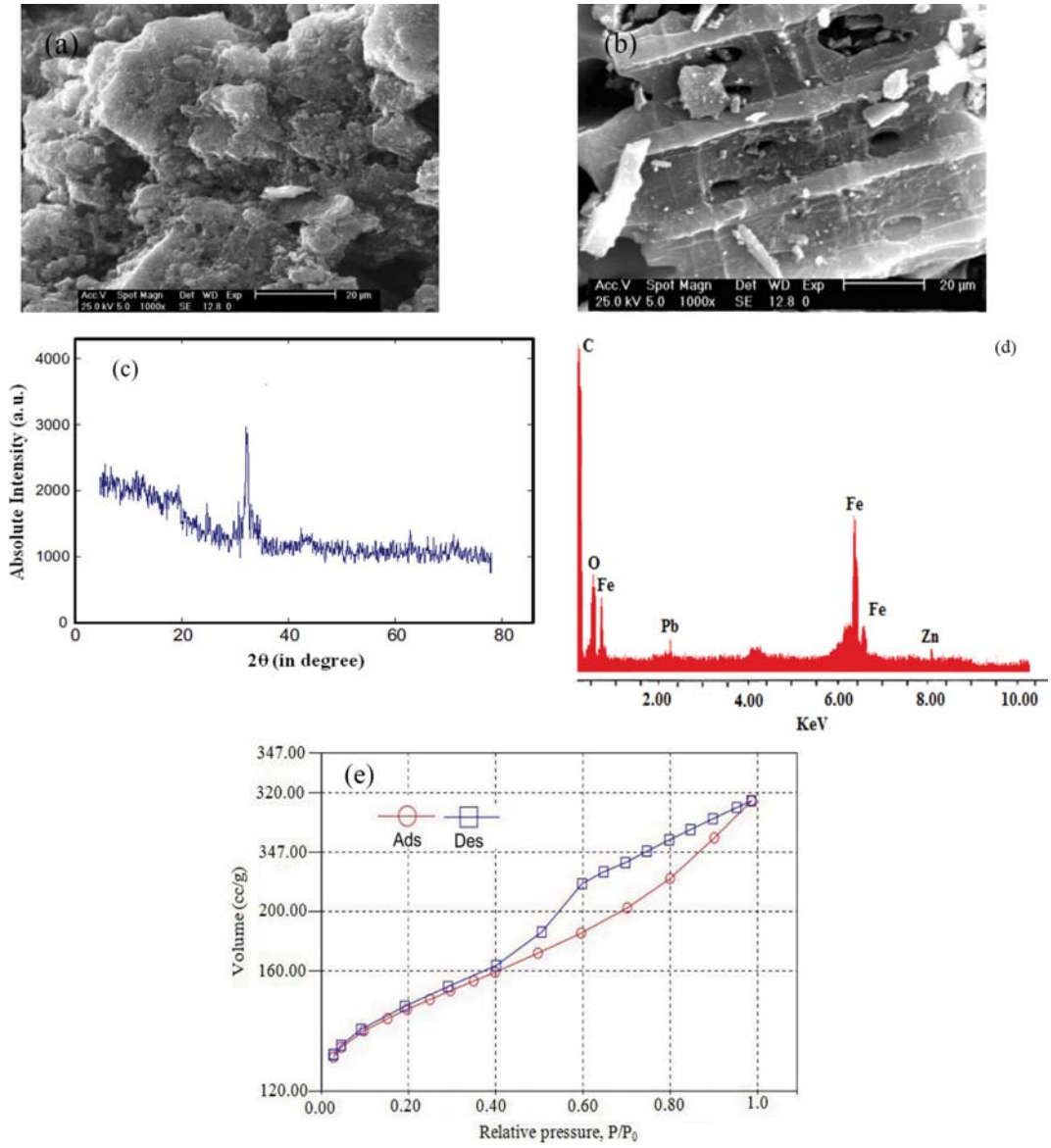

Fig. 1. SEM images of (a) pure PAC and (b) PAC/Fe_3O_4, XRD diagrams of PAC/Fe_3O_4 (c), EDAX spectrum (d) and (e) BET.

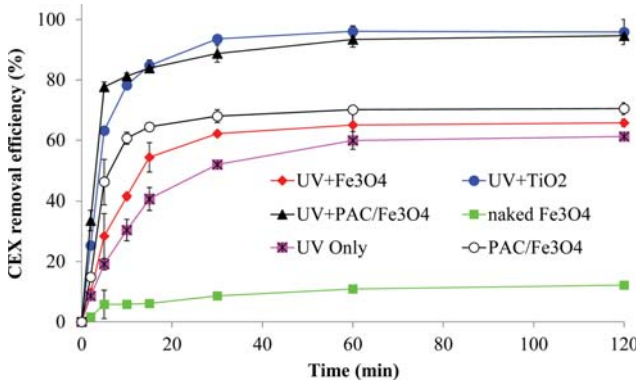

Fig. 2. A comparative study of CEX removal using UV only, naked Fe_3O_4, UV/Fe_3O_4, UV+TiO_2, PAC/Fe_3O_4 and UV+PAC/Fe_3O_4 (solution pH 7.0, catalyst dosage 1.0 g/L and initial CEX concentration 25 mg/L).

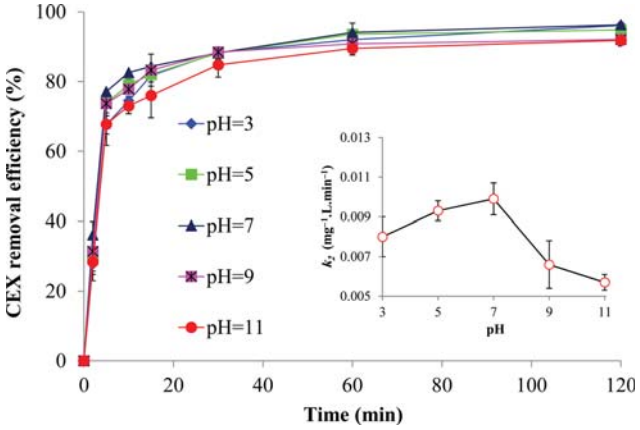

Fig. 3. The effect of solution pH on the photocatalytic removal of CEX from aqueous solution (catalyst dosage 1.0 g/L and initial CEX concentration 25 mg/L).

which is a useful tool for study of its crystalline feature, is shown in Fig. 1(c). Based on the XRD diagram prepared in the 2θ of 10-70°, a narrow diffraction peak is observed at 2θ of 35.5° which belongs to magnetite particles, proving its presence in the structure of activated carbon. Furthermore, the results of elemental analysis are represented in EDAX spectrum of PAC/Fe_3O_4 in (Fig. 1(d)), demonstrating that 71.6, 8.3 and 20.1% of the composite structure is included carbon, oxygen and iron, respectively. However, the remaining part (28%) can be attributed to the magnetite particles. Results of BET analysis revealed that PAC/Fe_3O_4 surface area is about 671.2 m^2/g. Moreover, the adsorption/desorption isotherms of PAC/Fe_3O_4 are illustrated in (Fig. 1(e)), which show that the type IV isotherm for the synthesized composite, based on IUPAC. This finding confirms that PAC/Fe_3O_4 has mesoporous structure [22].

2. A Comparative Study

A comparative study of CEX removal using UV only, naked Fe_3O_4, UV/Fe_3O_4, UV+TiO_2, PAC/Fe_3O_4 and UV+PAC/Fe_3O_4 (Fig. 2) shows the results of CEX removal during 120 min with 1 g/L PAC/Fe_3O_4 dosage, pH of 7 and 25 mg/L CEX concentration. Having a closer look at the figure, the maximum amount of CEX removal was obtained by UV+PAC/Fe_3O_4 and UV+TiO_2 with about 95% removal efficiency. However, the minimum amounts of CEX removal were only 12.2 and 61.2% which were obtained via the application of bare Fe_3O_4 and UV only, respectively. This means that bare Fe_3O_4 and UV cannot only provide the removal efficiency of CEX, implying that CEX cannot be removed effectively by bare Fe_3O_4 and UV-light alone. In addition, the adsorption of CEX on the surface of PAC/Fe_3O_4 could remove 70.48% of CEX in aqueous solution. Herein, high adsorption capacity of PAC/Fe_3O_4 may be due to the porous structure of composite and also its high surface area. In addition, the simultaneous application of UV light and Fe_3O_4 in UV/Fe_3O_4 was relatively similar to PAC/Fe_3O_4 (65.8%). Therefore, among all the applied processes, we selected UV+PAC/Fe_3O_4 and UV+TiO_2 as most effective processes of CEX removal for the next experiments. These results suggest good photocatalytic activity for as-synthesized composite and TiO_2 on CEX removal in the presence of UV light. Also, it can be concluded that the PAC/Fe_3O_4 and UV+TiO_2 have a synergistic effect when simulated by UV, and consequently CEX removal efficiency is enhanced compared to PAC/Fe_3O_4 and UV alone. This synergistic effect is assigned to the formation of reactive species ($HO^{\bullet}$) for CEX degradation. High removal efficiency of CEX by UV+PAC/Fe_3O_4 and UV+TiO_2 systems can be explained by the simultaneous presence of adsorption and degradation processes. Similar observations have been reported previously by other studies as presented in the literature [23,24].

3. Effect of Experimental Variables

3-1. Effect of Solution pH

pH of aqueous solution is an effective factor in photocatalytic removal of antibiotics from aqueous solution. To study the role of solution pH on CEX removal, pH range varied between 3 to 11 and the other experimental variables were 120 min reaction time, 1 g/L catalyst dosage and 25 mg/L initial CEX concentration. Results of pH studies are represented in (Fig. 3), indicating that at all pH values the photocatalytic removal of CEX are over 90%. In fact, by increasing solution pH from 3 to 7, photocatalytic removal of CEX reached to a peak which was followed by decreasing by enhancement of pH of solution to 11. Therefore, pH 7 was considered as an optimum pH value for the subsequent experiments, which is quite similar to the pH of real wastewaters. At pH values >7.0, low removal rate of CEX might be attributed to the electrostatic repulsion between CEX molecules and the surfaces of the composite, due to increasing the magnitude of negative charges on CEX and PAC-Fe_3O_4, and subsequently reducing the adsorption efficiency. Thus, when solution pH enhanced, the number of negatively charged sites on composite was improved, which caused promotion of the repulsion forces between CEX molecules and the beads surface. Based on the zero point of charge (pH_{pzc}) of PAC/Fe_3O_4, its surface areas are positively charged at low pH values and negatively charged at high pH values [16]. Furthermore, since CEX has amphoteric features and its pH_{pzc} are 4.5 and 5, CEX has high affinity to adsorb onto PAC/Fe_3O_4 at pH>5 values. In addition, although an increase in solution pH from 3 to 7 and 7 to 11 led to an insignificant increase and decrease in CEX removal efficiency, respectively, the effect of pH on kinetic rate constant was significant. By increasing pH from 3 to 7 and 7 to 11, K showed 24% increase and 42% decrease, respectively.

The reaction time is a critical experimental parameter in photo-

catalytic reactions, due to its significant influence on the cost and efficiency of a system. According to Fig. 3, the photocatalytic reaction is very high at first steps of the experiment, which may be attributed to the high pores and cavities on the surfaces of PAC/Fe_3O_4 leading to the production of high number of $^{\bullet}OH$ and $^{\bullet}O_2$ radicals [25]. Indeed, after passing 15 and 60 min, over 80 and 90% of the initial CEX concentration was removed, respectively. However, during 60 to 120 min of reaction, no significant changes were seen in removal of CEX in the UV+PAC/Fe_3O_4 system. This finding can be ascribed to the filling of surfaces of PAC/Fe_3O_4 that prevents contact between UV light and PAC/Fe_3O_4 leading to a decrease in the production of $^{\bullet}OH$ and $^{\bullet}O_2$ radicals and consequently removal efficiency of CEX [26,27]. However, as reaction time increased, the CEX removal efficiency showed insignificant increase, due to the competition between adsorbate molecules and hydroxyl radicals ($^{\bullet}OH$) to occupy the surface sites [28]. The obtained results revealed a sharp increase in photocatalytic removal of CEX using UV only, TiO_2 only, H_2O_2 only and UV+TiO_2+H_2O_2 with increasing the reaction time [29].

3-2. Effect of Catalyst Dosage

The catalyst dosage extremely affects the removal efficiency of pollutants in a photocatalytic system. The results of the effect of different catalyst dosages (0.1-2 g/L) on photocatalytic removal of CEX at solution pH of 7, 120 min reaction time and 25 mg/L initial CEX concentration are given in Fig. 4. As can be seen, increasing catalyst dosage from 0.1 to 1.0 g/L led to the improvement of CEX photocatalytic removal from 62.81 to 95.2%. The overall surface reactive sites of catalyst increases with enhancing catalyst dosage. In addition, at higher dosages of catalyst, more Fe_3O_4 nanoparticles react with UV; subsequently, the production rate of reactive species significantly increased in the system [30]. Similar results were reported by Babaei et al. [31] on photocatalytic degradation of nonylphenol using ZnO particles [31]. Furthermore, findings of Kord Mostafapour et al. [32] showed a direct relationship with ciprofloxacin photodegradation from aqueous solution using copper oxide nanoparticles with catalyst dosage [32]. However, by increasing catalyst dosage from 1 to 2 g/L, only 2.67% increase was observed in photocatalytic CEX removal, which can be attributed to dropping the penetration of UV light, due to the enhanced scattering effect in the aqueous solution. However, with enhancement of catalyst dosage between 1 and 2 g/L, K increased by 2.4 orders of magnitude. Therefore, 1 g/L was chosen as an optimum dosage of catalyst and applied in the next coming experiments.

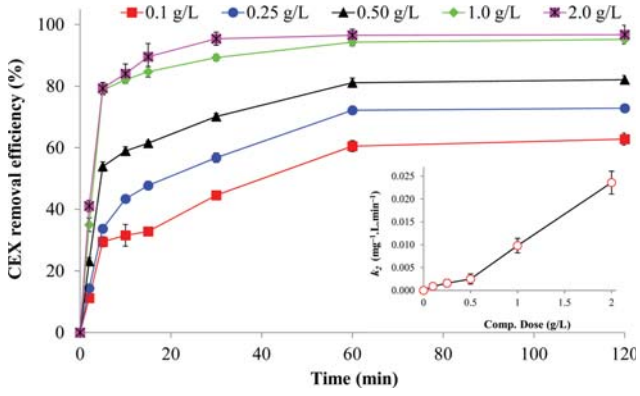

Fig. 4. The effect of catalyst dosage on the photocatalytic removal of CEX from aqueous solution (solution pH 7.0 and initial CEX concentration 25 mg/L).

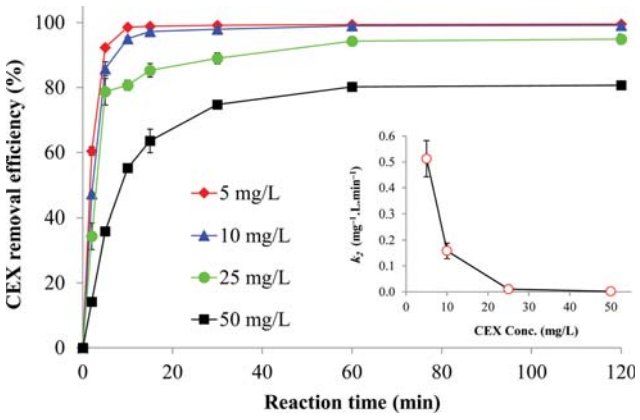

Fig. 5. The effect of initial CEX concentration on the photocatalytic removal of CEX from aqueous solution (solution pH 7.0 and catalyst dosage 1.0 g/L).

3-3. Effect of Initial CEX Concentration

One of the most influential experimental agents on the photocatalytic removal of contaminants is their initial concentration in the solution. Hence, photocatalytic degradation of CEX was studied at various initial CEX concentrations of 5, 10, 25 and 50 mg/L and pH of 7 and 1 g/L adsorbent dosage. The obtained results of experiments are illustrated in Fig. 5. Accordingly, photocatalytic degradation of CEX witnessed a significant decline with increasing initial CEX concentration from 5 to 50 mg/L. In fact, at specific catalyst dosage, an increase in the initial contaminant concentrations will lead to decreasing its photocatalytic removal. This observation can be ascribed to this reason, that by increasing pollutant molecules, the surface reactive sites will be occupied which prevents releasing hydroxyl ions (OH^-). Furthermore, these molecules hamper the presence of OH^-, O_2^- and Fe^{2+} on the surfaces of catalyst [33]. So, increasing photocatalytic removal of CEX can be derived from consumption of free radicals [34]. Another reason for this phenomenon is the direct relationship with CEX concentration with filling surface reactive sites, which decreased light penetration to the catalyst surfaces, causing a decrease in activation of catalyst molecules [35]. In addition, results of kinetic studies showed that a sharp decline was observed in second-order kinetic rate constant of CEX from 0.5129 to 0.0014 $mg^{-1}\cdot L\cdot min^{-1}$ with increasing CEX concentration from 5 to 50 mg/L, respectively.

Among all the models applied for describing photocatalysis kinetics, the Langmuir-Hinshelwood (L-H) model is the most common one [36,37]:

$$k = \frac{K_{CEX} k_c}{1 + K_{CEX}[CEX]_o} \tag{12}$$

Equation below shows the linearized form of Eq. (12):

$$\frac{1}{k} = \frac{1}{k_c}[CEX]_o + \frac{1}{k_c K_{CEX}} \tag{13}$$

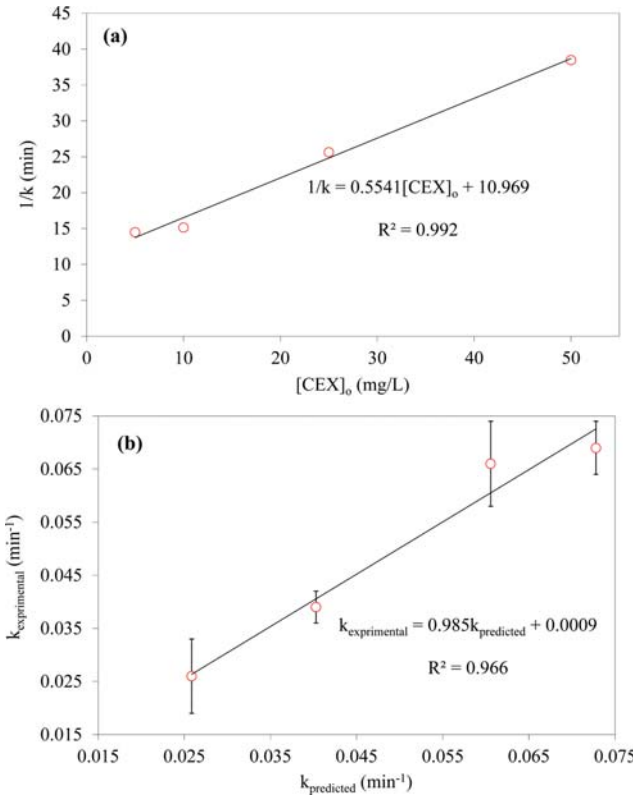

Fig. 6. (a) Langmuir-Hinshelwood (L-H) kinetic model of CEX photocatalytic degradation (b) comparison between experimental and calculated first-order rate constants for the photocatalytic oxidation of CEX (pH 7.0, catalyst dosage 1.0 g/L and initial CEX concentration 5-50 mg/L).

where, k represents the first-order rate constant, k_c represents the rate constant of surface reaction (mg min^{-1}) and K_{CEX} represents the L-H adsorption constant of CEX over PAC/Fe_3O_4 surface (mg^{-1}) in solution. An admissible linear correlation (R^2=0.992) between 1/k and $[CEX]_o$ given in Fig. 6(a) shows the considerable adsorption of CEX on PAC/Fe_3O_4. Surface reactions of CEX, like oxidation by surface, are critical. The obtained values for k_c and K_{CEX} were 1.805 mg min^{-1} and 0.051 mg^{-1}, respectively. As the process of CEX degradation takes place on the surfaces of PAC/Fe_3O_4, any decrease in recombination of electron-hole pair will lead to increasing the photocatalytic removal of CEX. An efficient trapping of electrons enables reactions of valence band holes (h^+_{vb}) with species adsorbed over the PAC/Fe_3O_4 surface. Fig. 6(b) illustrates the values of first-order rate constant obtained theoretically against experimentally with a relatively high coefficient of correlation (R^2=0.966).

Table 1. Isotherm parameters of CEX adsorption onto the surfaces of PAC/Fe_3O_4

Model	Parameter	Value
Langmuir	q_m (mg/g)	114.9
	K_L (L/mg)	0.133
	R_L	0.23
	R^2	0.967
Freundlich	K_F (mg/g(Lmg)1/n)	13.3
	n (–)	1.35
	R^2	0.914
Temkin	K_T (mg g^{-1} $min^{-0.5}$)	1.22
	B	31.7
	A_T	78.1
	R^2	0.700
Dubinin-Radushkevich	k_{ad} (mol^2/kJ^2)	4.2×10^{-7}
	q_s (mg/g)	47.5
	E (kJ/mol)	1.1
	R^2	0.896

4. Equilibrium of Adsorption Studies

In this study, CEX adsorption data were fitted on four isotherm models and the graphs of studied model. In addition, the obtained model coefficients with related coefficients of determination (R^2) are reported in Table 1. As illustrated in Table 1, among all the four applied models, Freundlich and Langmuir had highest coefficients of determination (R^2>0.9), indicating their high ability to fit the data of CEX adsorptive removal. However, since R^2 of Langmuir was apparently higher than that of Freundlich, it can be postulated that Langmuir has higher capability of fitting CEX removal data than Freundlich. Table 2 shows the adsorption capacity of some selected adsorbents in the literature for removal of CEX from solution. Having a closer look, the applied adsorbent, compared to the other studied adsorbents, has high adsorption capacity of CEX removal. Furthermore, parameter "R_L" in the Langmuir model is less than 1, which shows that the process of CEX adsorption onto the surfaces of PAC/Fe_3O_4 is favorable. Moreover, according to Table 1, the Temkin model did not represent significant R^2, representing low correlation with the data of CEX removal. While, R^2 of D-R model (0.89) was more significant than Temkin model. Furthermore, based on parameter E in D-R model which is 1.1, it can be concluded that the process of adsorption is physical.

5. Degradation Kinetic Studies

Results of CEX degradation kinetic studies with UV+PAC/Fe_3O_4

Table 2. Comparison of the maximum adsorption capacities some selected adsorbents in the literature for removal of CEX from solution

Antibiotic	Adsorbent	Equilibrium adsorption (mg/g)	Reference
CEX	Activated carbon nanoparticles	7.080	Pouretedal et al. [38]
CEX	Bentonite	10.38	Al-Khalisy et al. [39]
CEX	NZ	16.10	Samarghandi et al. [40]
	CZ	24.50	
CEX	PAC/Fe_3O_4	114.9	This study

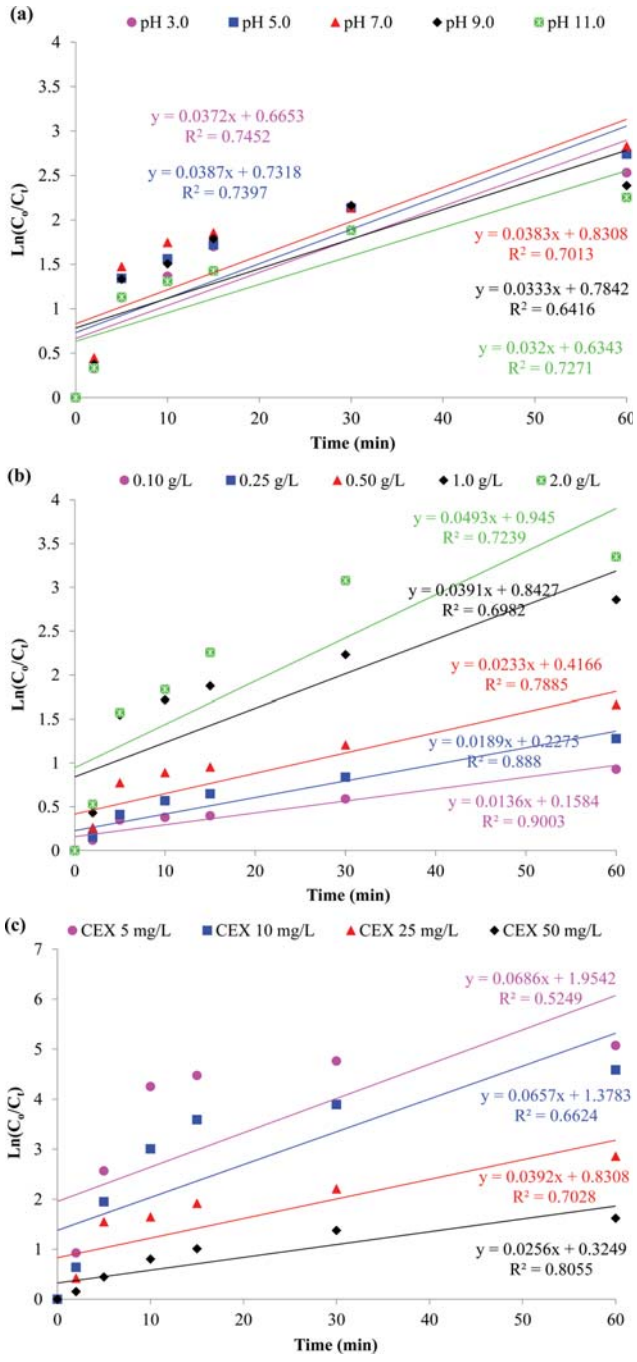

Fig. 7. First-order kinetic model of CEX photocatalytic removal from aqueous solution at different pH of solution (a), adsorbent dosages (b) and initial CEX concentrations (c).

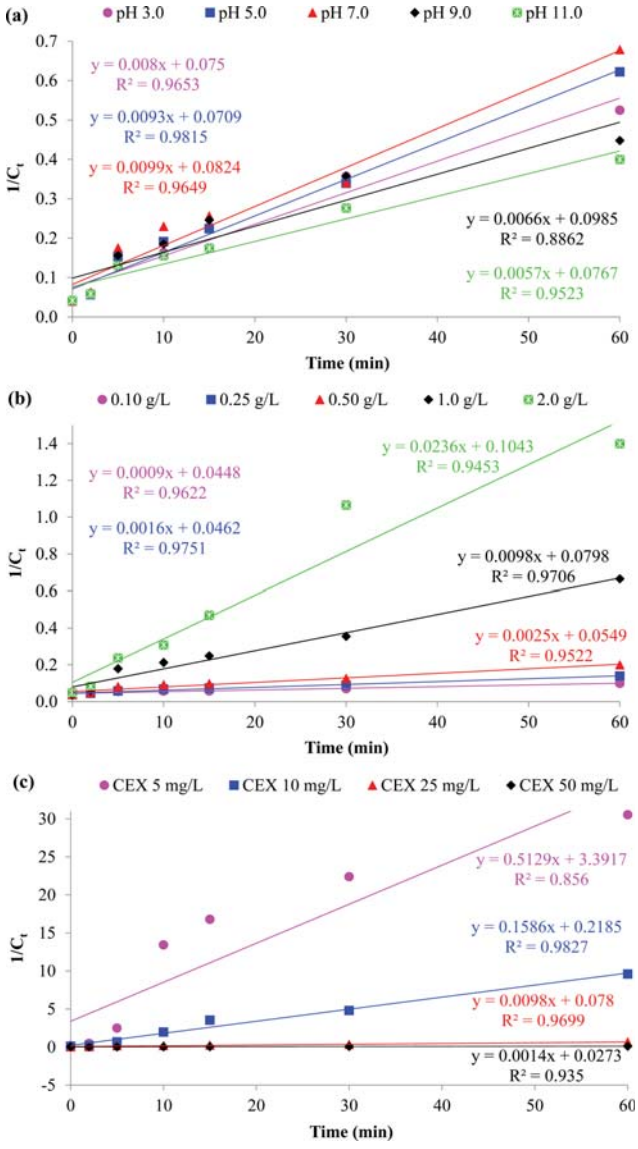

Fig. 8. Second-order kinetic model of CEX photocatalytic removal from aqueous solution at different pH of solution (a), adsorbent dosages (b) and initial CEX concentrations (c).

process are illustrated in (Figs. 7-8) which show the good fitting of the experimental data of CEX removal with the applied models. Furthermore, the kinetic experiments were conducted in 60 min equilibrium time obtained from the preliminary experiments. The coefficient of determination (R^2), as a reliable index for evaluation of the efficiency of model, and related parameters are reported in Table 3. Apparently, higher values of R^2 represent the higher ability of the model for fitting the experimental data. Based on Table 3, the quantities of k_1 and k_2 in first-order and second-order, respectively, had a fluctuating trend with increasing solution pH. However, different results were observed in the case of adsorbent dosage. Indeed, by increasing adsorbent dosage from 0.1 to 2 g/L, the amount of k_1 and k_2 improved from 0.014 to 0.049 min^{-1}, and 0.0009 to 0.0236 $mg^{-1}\cdot L\cdot min^{-1}$, respectively, although some fluctuations happened. These observations prove that the photocatalytic removal of CEX using UV+PAC/Fe_3O_4 is a pH-dependent and concentration-dependent process. Moreover, an indirect relationship was seen between k_1 and k_2 and initial CEX concentration. Ultimately, among the studied kinetic models, second-order model, compared to first-order model, had better correlation with the data of CEX removal at different pH of solution, adsorbent dosage and initial CEX concentrations.

6. Scavenging Experiments

To prove the photocatalytic removal of CEX using the synthe-

Table 3. Kinetic parameters of CEX removal at different experimental variables

Experimental factor		First-order		Second-order	
		k_1	R^2	k_2	R^2
pH of solution	3	0.037	0.745	0.008	0.965
	5	0.039	0.74	0.0093	0.982
	7	0.038	0.701	0.0099	0.965
	9	0.033	0.642	0.0066	0.886
	11	0.032	0.727	0.0057	0.952
Adsorbent dosage (g/L)	0.1	0.014	0.9	0.0009	0.962
	0.25	0.019	0.888	0.0016	0.975
	0.50	0.023	0.789	0.0025	0.952
	1	0.039	0.698	0.0098	0.971
	2	0.049	0.724	0.0236	0.945
Initial CEX concentration (mg/L)	5	0.069	0.525	0.5129	0.856
	10	0.066	0.662	0.1586	0.983
	25	0.039	0.703	0.0098	0.97
	50	0.026	0.806	0.0014	0.935

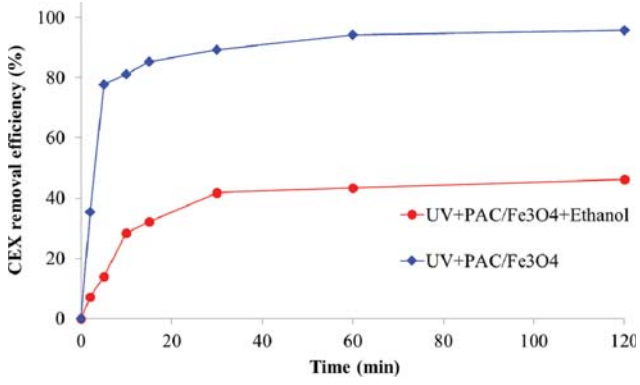

Fig. 9. Effect of scavengers on photocatalytic removal of CEX (solution pH 7.0, catalyst dosage 1.0 g/L and initial CEX concentration 25 mg/L).

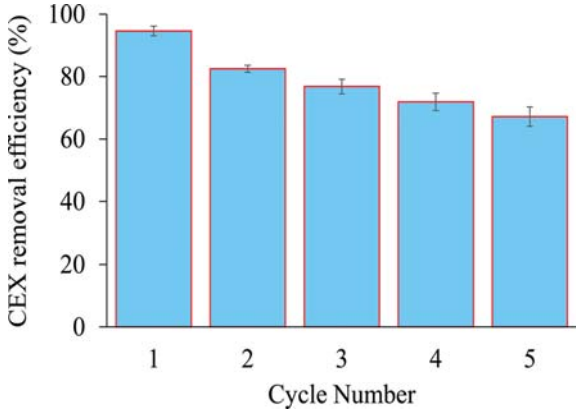

Fig. 10. The study on photocatalytic removal of CEX at five consecutive cycles.

sized catalyst via production of $^{\bullet}OH$ radicals, ethanol was used as a scavenger. The experiments were at pH 7, catalyst dosage 1 g/L and 25 mg/L CEX concentration. Results revealed that addition of ethanol to experiments caused a significant decrease in CEX removal efficiency from 95.7 to 46%. In addition, the first- and second-order rate constants decreased from 0.0099 to 0.0005 and 0.039 to 0.009, respectively (Fig. 9). A sharp decrease in CEX removal efficiency with addition of ethanol would be due to declining hydroxyl radical activities, which shows that these radicals were created in UV+PAC/Fe_3O_4.

7. Reusability of Catalyst

The possibility of reusability and regeneration of the applied catalyst is practically critical. So, we studied the catalyst reusability during a five successive use cycle process. In brief, after ending each cycle of use, an external magnet was used for separation of catalyst, which was followed by washing with DI water, drying in an oven at 80 °C for 2 h and reusing for the subsequent cycle. Results of regeneration study are also illustrated in Fig. 10. According to the figure, the photocatalytic removal efficiency of CEX represented a decreasing trend from cycle 1 to 5. Thus, around 94.60% of CEX was removed at cycle 1, decreasing to 67.16% after the fifth cycle, which indicates that PAC/Fe_3O_4 is a reusable catalyst. The reduction of photocatalytic CEX removal can be ascribed to the loss of catalyst mass and lack of perfect performance in removal of residual by-products into the pores and spaces of catalyst surface. Furthermore, this relatively low reduction in CEX removal, which is derived from the high reusability of catalyst, may lead to decreasing operation cost of the photocatalysis system.

CONCLUSION

Photocatalytic degradation of CEX was performed in a UV+PAC/Fe_3O_4 system at different experimental conditions. The synthesized catalyst could apparently enhance the efficiency of photocatalysis system, in comparison with UV only and the adsorption system. In addition, the maximum amount of photocatalytic CEX removal was obtained at pH 7 and 60 min contact time. The removal of CEX showed an increasing trend with enhancing catalyst dosage.

While, by increasing initial CEX concentration, the CEX removal decreased significantly. The findings of kinetic studies revealed that the photocatalytic removal of CEX is a pH-dependent and concentration-dependent process, which has the highest correlation with pseudo second-order, compared to first-order model. Results of isotherm studies by Langmuir-Hinshelwood (L-H) model showed that the process of CEX degradation was carried out on the surfaces of catalyst. Moreover, addition of ethanol caused a significant decline in CEX removal efficiency, due to decreasing hydroxyl radical production. In addition, from the reusability experiments, it was observed that PAC/Fe_3O_4 is a reusable catalyst without a significant loss in its performance after five consecutive cycles of use. Ultimately, based on the results of this study, it is concluded that PAC/Fe_3O_4 not only has high adsorption capacity of CEX removal, but also can play the role of a reliable catalyst for photocatalytic removal of CEX from aqueous solution.

ACKNOWLEDGEMENT

This article was derived from M.Sc. degree thesis of Miss. Forough Gashtasbi. The authors of this paper are sincerely grateful to Ahvaz Jundishapur University of Medical Sciences Dr. Ali Akbar Babaei for their academic support.

AUTHORS' CONTRIBUTIONS

The authors declare that they have no conflict of interest. All authors have read and approved the final version of the manuscript.

REFERENCES

1. G. Nazari, H. Abolghasemi and M. Esmaieli, *J. Taiwan Institute. Chem. Eng.*, **58**, 357 (2016).
2. Z. Fang, J. Chen, X. Qiu, W. Cheng and L. Zhu, *Desalination*, **268**(1), 60 (2011).
3. F. Ay ana F. Kargi, *J. Hazard. Mater.*, **179**(1), 622 (2010).
4. Z. Aksu and Ö. Tunç, *Process Biochemistry*, **40**(2), 831 (2005).
5. D. Dimitrakopoulou, I. Rethemiotaki, Z. Frontistis, N. P. Xekoukoulotakis, D. Venieri and D. Mantzavinos, *J. Environ. Manage.*, **98**, 168 (2012).
6. A. Mohseni-Bandpi, T. J. Al-Musawi, E. Ghahramani, M. Zarrabi, S. Mohebi and S. A. Vahed, *J. Mol. Liq.*, **218**, 615 (2016).
7. A. R. Khataee, M. N. Pons and O. Zahraa, *J. Hazard. Mater.*, **168**(1), 451 (2009).
8. K. Sahel, N. Perol, F. Dappozze, M. Bouhent, Z. Derriche and C. Guillard, *J. Photochem. Photobio. A: Chem.*, **212**(2), 107 (2010).
9. L. Gu, Z. Chen, C. Sun, B. Wei and X. Yu, *Desalination*, **263**(1), 107 (2010).
10. M. R. Delsouz Khaki, M. S. Shafeeyan, A. A. Abdul Raman and W. M. Ashri Wan Daud, *J. Mol. Liq.*, **258**, 354 (2018).
11. D. Du, W. Shi, L. Wang and J. Zhang, *Appl. Catal. B: Environ.*, **200**, 484 (2017).
12. A. A. Babaei, A. Azari, R. R. Kalantary and B. Kakavandi, *Water Sci. Technol.*, **72**, 1988 (2015).
13. S. Yang, T. Xiao, J. Zhang, Y. Chen and L. Li, *Sep. Purif. Technol.*, **143**, 19 (2015).
14. H. Lan, A. Wang, R. Liu, H. Liu and J. Qu, *J. Hazard. Mater.*, **285**, 167 (2015).
15. S. Jorfi, B. Kakavandi, H. R. Motlagha, M. Ahmadi and N. Jaafarzadeh, *Environ.*, **219**, 216 (2017).
16. B. Kakavandi, M. Jahangiri-rad, M. Rafiee, A. R. Esfahani and A. A. Babaei, *Micropor. Mesopor. Mater.*, **231**, 192 (2016).
17. I. Langmuir, *J. Franklin. Ins.*, **183**(1), 102 (1917).
18. H. M. F. Freundlich, *J. Phys. Chem.*, **57**(385), e470 (1906).
19. O. Celebi, Ç. Üzüm, T. Shahwan and H. N. Erten, *J. Hazard. Mater.*, **148**(3), 761 (2007).
20. N. D. Hutson and R. T. Yang, *Adsorption*, **3**(3), 189 (1997).
21. Y. Xu and D. Z. Zhao, *Water Res.*, **41**(10), 2101 (2007).
22. M. Balsamo, T. Budinova, A. Erto, A. Lancia, B. Petrova, N. Petrov and B. Tsyntsarski, *Sep. Purif. Technol.*, **116**, 214 (2013).
23. H. Mehrizadeh, A. Niaei, H. H. Tseng, D. Salari and A. Khataee, *J. Photochem. Photobio. A: Chem.*, **332**, 188 (2017).
24. S. Gao, C. Guo, S. Hou, L. Wan, Q. Wang, J. Lv, Y. Zhang, J. Gao, W. Meng and J. Xu, *J. Hazard. Mater.*, **331**, 1 (2017).
25. K. Tyrovola, E. Peroulaki and N. P. Nikolaidis, *Eur. J. Soil Bio.*, **43**(5), 356 (2007).
26. T. D. Nguyen, N. H. Phan, M. H. Do and K. T. Ngo, *J. Hazard. Mater.*, **185**, 653 (2011).
27. W. Wang, Y. Liu, T. Li and M. Zhou, *Chem. Eng. J.*, **242**, 1 (2014).
28. M. Behrouzi-Navid, M. Olya and K. Monakchian, The 5th National Conference and Exhibition on Environ. Engine., Tehran, Iran (2011).
29. P. Bansal, A. Verma, K. Aggarwal, A. Singh and S. Gupta, *Canadian J. Chem. Eng.*, **94**(7), 1269 (2016).
30. A. J. Jafari, B. Kakavandi, N. Jaafarzadeh, R. R. Kalantary, M. Ahmadi and A. A. Babaei, *J. Ind. Eng. Chem.*, **45**, 323 (2017).
31. A. A. Babaei, A. R. Mesdaghiniai, N. Jaafarzadeh Haghighi, R. Nabizadeh and A. H. Mahvi, *J. Hazard. Mater.*, **185**, 1273 (2011).
32. F. Kord Mostafapour, E. Bazrafshan, D. Belarak and N. Khoshnamvandi, *Rafsanjan Univ. Med. Sci.*, **15**(4), 307 (2016).
33. C. Cai, H. Zhang, X. Zhong and L. Hou, *J. Hazard. Mater.*, **283**, 70 (2015).
34. A. Jonidi Jafari, B. Kakavandi, N. Jaafarzadeh, R. R. Kalantary, M. Ahmadi and A. A. Babaei, *J. Ind. Eng. Chem.*, **45**, 323 (2017).
35. M. Golshan, M. Zare, Gh. Goudarzi, M. Abtahi and A. A. Babaei, *Mater. Res. Bulletin*, **91**, 59 (2017).
36. Y. Yao, L. Wang, L. Sun, S. Zhu, Z. Huang, Y. Mao, W. Lu and W. Chen, *Chem. Eng. Sci.*, **101**, 424 (2013).
37. M. A. Behnajady, N. Modirshahla and R. Hamzavi, *J. Hazard. Mater.*, **133**, 226 (2006).
38. H. R. Pouretedal and N. Sadegh, *J. Water Process. Eng.*, **1**, 64 (2014).
39. R. S. Al-Khalisy, M. A. A. Al-Haidary and A. H. Al-Dujaili, *Sep. Sci. Technol.*, **45**, 1286 (2010).
40. M. R. Samarghandi, T. J. Al-Musawi, A. Mohseni-Bandpi and M. Zarrabi, *J. Mol. Liq.*, **211** 431 (2015).